# Innovative bidirectional video-goniophotometer combining transmission and reflection measurements

*Marilyne Andersen, Christian Roecker, Jean-Louis Scartezzini*
*Solar Energy and Building Physics Laboratory (LESO-PB), Swiss Federal Institute of Technology (EPFL), CH - 1015 Lausanne, Switzerland*

**This paper describes the design process and setting up of a novel bidirectional goniophotometer, relying on digital imaging and allowing the combination of transmission and reflection measurements. As its measurement principle is based on the projection of the emerging light flux on a rotating diffusing screen towards which a calibrated CCD camera is pointed (used as a multiple-points luminance-meter), several strong constraints appear in reflection mode due to the conflict of incident and emerging light flux: for five out of the six screen positions (unless incidence is normal), the incident beam must penetrate in a way that it is restricted to the sample area only; in addition to this, when the screen obstructs the incoming light flux, a special opening in the latter is required as well to let the beam reach the sample. The practical answer to these constraints, detailed in this paper, proved to be reliable, appropriate and efficient.**

## Introduction

To allow the integration of advanced daylighting systems in buildings and benefit from their potential as energy-efficient strategies, a detailed knowledge of their directional optical properties is necessary. These properties are accurately described by the Bidirectional Transmission (or Reflection) Distribution Function, abbreviated BT(or R)DF, that expresses the emerging light flux distribution for a given incident beam direction (Commission Internationale de l'Eclairage, 1977). An original experimental method for their assessment, illustrated in Figure 1 was first developed for transmission measurements (Andersen et al., 2001): the light emerging from the sample is reflected by a diffusing triangular panel towards a CCD camera, which provides a picture of the screen in its entirety. Within six positions of the screen and camera around the sample (each separated by a 60° rotation from the next one), a complete investigation of the transmitted or reflected light is achieved.

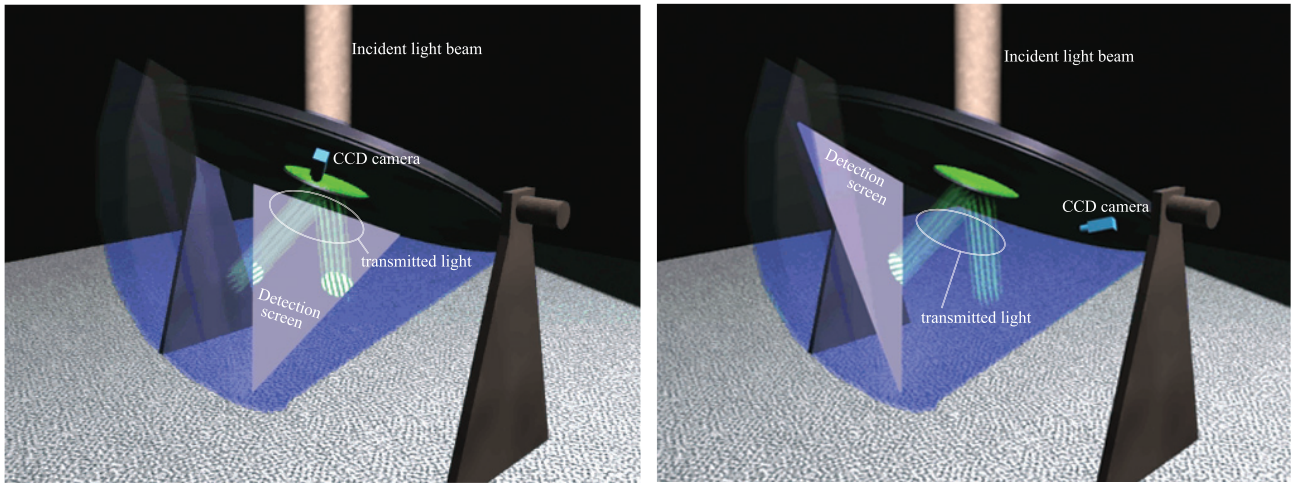


*(a) Arbitrary screen position p* *(b) Screen position p+1*

*Figure 1: Detection of transmitted light flux for two consecutive screen positions p and p+1.*

This innovative approach brought several major advantages when compared to characterization techniques requiring a sensor to be moved from one position to the other (Papamichael et al., 1988; Bakker and van Dijk, 1995; Aydinli, 1996; Breitenbach and Rosenfeld, 1998; Apian-Bennewitz and von der Hardt, 1998): a significant reduction of the BT(R)DF data assessment time (a few minutes instead of hours per incident direction) and a continuous information about the transmission (reflection) hemisphere, whose resolution is only limited by the pixellisation of the images.

The camera is used as a multiple-points luminance-meter and calibrated accordingly. A luminance mapping of the projection screen is carried out by capturing images of it at different integration intervals, thus avoiding over and under-exposure effects, and appropriately combining the latter to extract BT(R)DF data at a pixel level resolution.
Material samples showing large range of luminances can thus be handled without any loss of accuracy, while an appreciable flexibility is allowed in the data processing (Andersen, 2004).

For BRDF measurements (reflection mode), however, additional constraints appear due to the conflict of incident and emerging light flux.
For five out of the six screen positions (unless incidence is normal), the detection principle can be kept identical as in transmission mode (Figure 2(a)), except that light flux must penetrate the measurement space in a way that the beam is restricted to the sample area only. As there is one position (all six for normal incidence) where the screen obstructs the incoming light flux, a special opening in the latter is required to let the beam reach the sample, producing a blind spot at that specific screen position (and only in reflection mode), as illustrated in Figure 2(b).
The design process of the instrument combining BTDF and BRDF measurements is presented in this paper, and the mechanical components specifically developed to answer to these constraints in a practical and efficient way are described.

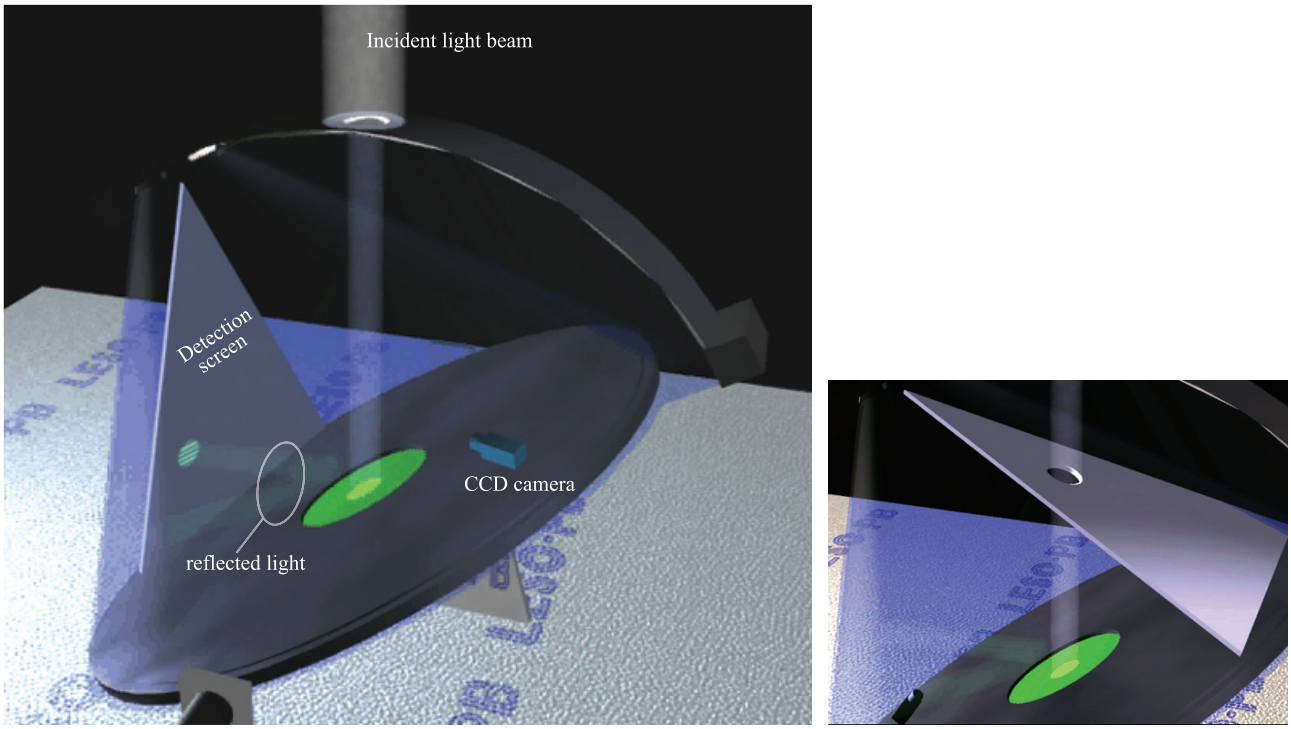


*(a) Unobstructed penetration* *(b) Screen hole*

*Figure 2: Detection of reflected light flux.*

## Design of the transmission / reflection device

The final concepts of the envelope and the screen are illustrated by the sequence of images given in Figure 3. In order to control precisely the illuminated sample area and thus minimize the parasitic reflections and blind zone, a quarter-circular frame supports a perforated sheet on which a motorized strip showing one circular aperture is unrolling, of diameter equal to the sample's and facing the light source for any incident altitude angle $\theta_1$. The sheet's elliptic openings are of dimensions given by the apparent sample surface (accounting for inclination angle $\theta_1$) and are correspondingly positioned on the quarter circle arc.

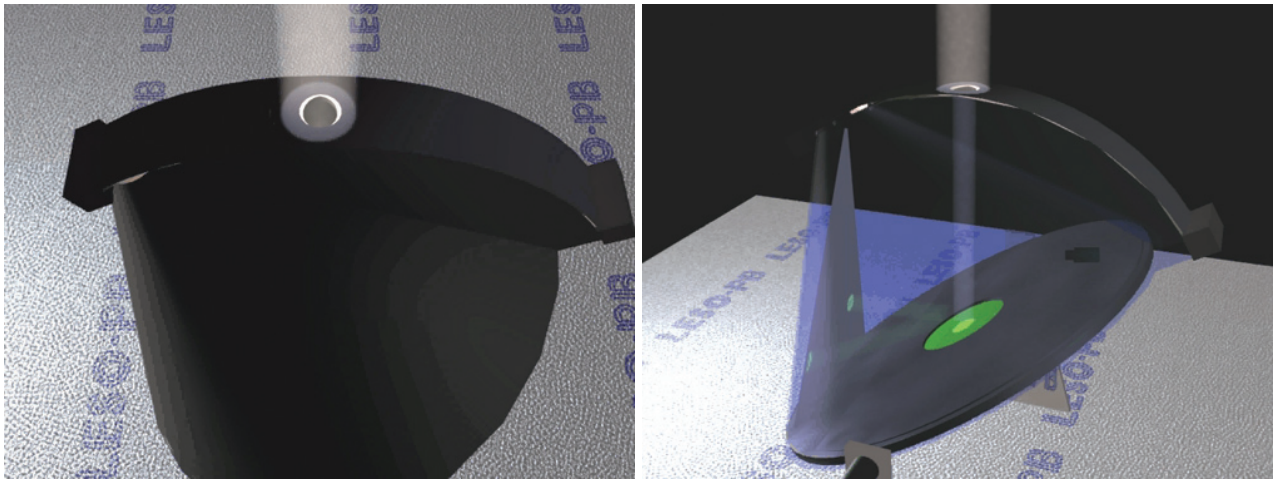

*(a) Strip hole over elliptic opening* *(b) Controlled illumination of sample*

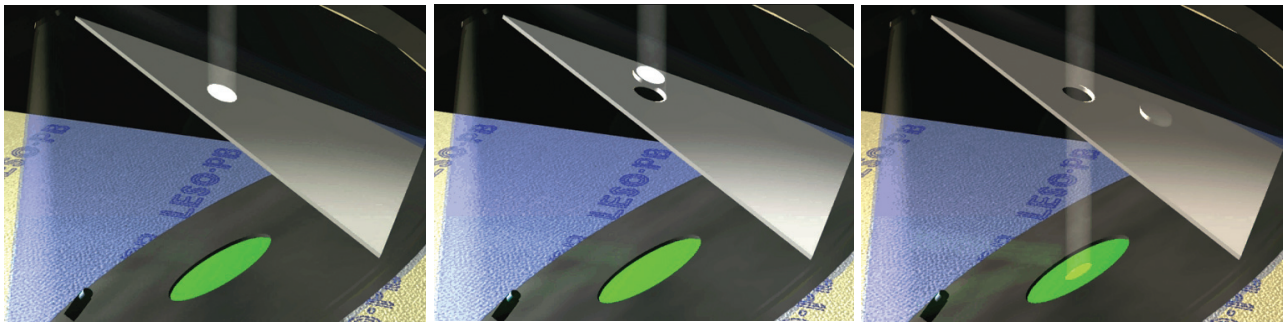

*(c) Obstructing screen* *(d) Lifting of cover* *(e) Removal from path*

*Figure 3: Control of incident beam penetration and path through obstructing screen.*

The projection screen concept relies on the removal of elliptic covers by a robotic mechanism. The ellipses' dimensions were again determined by the apparent sample area accounting for angle $\theta_1$, yet this time projected on a the screen surface, that is oblique to the sample plane with a tilt angle $\Theta_0 \cong 49.1°$. The induced blind spot can thus be exactly reduced to the light beam's area, which allows a minimal loss of information on the emerging light distribution and negligible parasitic reflections around the sample area. Of course, a blind spot only appears for one of the six screen positions, except for normal incidence where the tip needs to be removed for all of them.

The optimal combination of altitude step $\Delta\theta_1$ and sample diameter $D$ is determined on one hand by the device's geometry itself, and on the other hand by the minimal illuminated area required for advanced fenestration systems or coating materials characterizations; the minimal allowed sample diameter was thus found to be equal to 15 cm.

Once the concept's applicability in practice was verified, the new components were designed and constructed.

## Measurement space envelope

The measurement space envelope for combined BTDF and BRDF measurements, shown on Figure 4(a), consists of a carbon fiber cap strengthened by a structural metallic frame; this frame also supports a static stainless-steel perforated sheet on which a moving synthetic strip can glide. The role of the synthetic strip is to select the elliptic hole through which the incident light's path will be adequately controlled (according to altitude $\theta_1$); at the same time, it prevents light from entering the measurement space through any other opening. Its unique aperture is therefore circular, slightly larger than the largest ellipse (i.e. the one associated to normal incidence); the chosen 10° step in altitude ensures that a 15 cm diameter hole never overlaps two consecutive entrances.

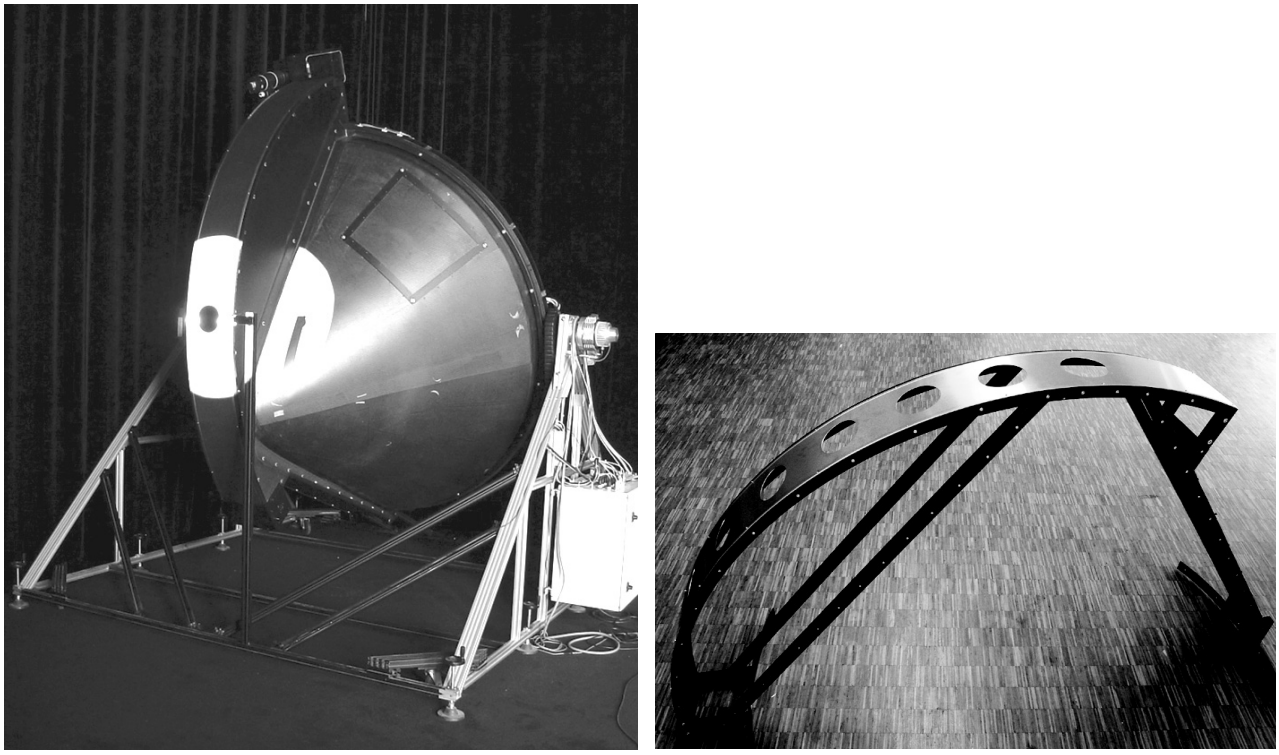

*(a) Goniophotometer in reflection mode* *(b) Metal sheet with cut-out ellipses*

*Figure 4: Structural components of the BT&RDF goniophotometer.*

The determination of the actual position and dimensions of the ellipses cut out from the metal sheet required a multiple stages process for an optimal incident light control:

- First, the theoretical geometric properties of the ellipses were determined based on trigonometric considerations, assuming a perfectly parallel beam reaching an elliptic surface of apparent horizontal axis 15 cm and vertical axis $15 \cdot \cos\theta_1$.
- Then, the ellipses dimensions were adjusted to the real incident beam, of imperfect collimation and thus producing blurred regions around the uniformly illuminated area, responsible for parasitic reflections. Once the optimal source distance was determined, different elliptic shapes were tried out to compare the achieved sample surface illumination. The most efficient compromise was established between optimal uniformity over the whole sample area and lower parasitic light flux; this was done for each ellipse individually, as more relative blurredness appeared for smaller ellipses. The determined shapes, cut out of cardboard sheets, were tested successfully; they led to only few percent of non-uniformly illuminated sample area while guaranteeing an

average relative blurredness area lower than 10%. It can be noted that these remaining parasitic reflections were reduced to a negligible level by adding a ring of highly absorbing material (“velvetine”) around the sample.

- Finally, the positions of the ellipses on the metal sheet had to account for the frame manufacturing imperfections (see above). The metal sheet was thus mounted temporarily on the frame, allowing to centre the ellipses thanks to a plumbline course driven by a progressive platform inclination. Their positioning was thereafter verified by pointing a fixed laser on the central axis and tilting the device to get each ellipse’s centre coincident with the laser spot; this test showed that an appropriate accuracy was achieved ($\pm$ 0.05 cm deviation). Before sending the metal sheet for cutting out, these positions were adjusted to a flat configuration of the sheet (i.e. to its neutral fiber), to avoid slight shifts due to the sheet’s thickness.

The resulting perforated metal sheet is shown on Figure 4(b); its inside surface is covered with “velvetine” (reflection factor lower than 1%).

## Diffusing projection screen

The dimensions, positioning and coating characteristics of the triangular projection panel are detailed in (Andersen et al., 2001; Andersen, 2004): a diffusing white paint manufactured by LMT allows to obtain an almost lambertian surface (perfectly diffusing), with only a 2.6% difference to the theoretical model.
The removal of screen covers, necessary to perform BRDF measurements, aims at leaving the incident beam path free, while the controlling of its shape is taken care of by the ellipses cut out from the metal sheet.
To minimize the blind zones, these screen covers must present elliptic shapes as well. Their exact geometry was determined following a similar procedure as for the metal sheet:

- First, their theoretical dimensions and positions were deduced by trigonometry on the basis of the intersection of a perfectly parallel beam (reaching the sample at different $\theta_1$ angles) with the tilted detection surface (accounting for the shift between sample and detection screen base planes.

- Then, using on the results provided by the sample illumination analysis with the actual light source and on the metal sheet ellipses dimensions, adjusted horizontal and vertical axes for the screen ellipses were estimated, to which a 2 mm margin was added to avoid edge effects.

- After that, to determine the actual dimensions of the cut out covers, the thickness of the screen had to be taken into account; on the other hand, the covers insertion required a slant between the upper (external) and lower (internal) sides of the screen, chosen unique and equal to 20° to ease the screen manufacturing. To leave the beam’s passage free through a screen of significant thickness, larger upper ellipses are required when the angle between the incoming beam and the screen plane increases (i.e. when $\mid \theta_1 - \Theta_0 \mid$ increases). The ellipses were thus adjusted accordingly, depending on each one’s incident tilt angle.

- Finally, as the above adjustment was only necessary for the ellipses half farthest from the $\theta_1 = \Theta_0$ direction, their vertical axes (and thus the blind zones) were reduced by re-centering them to open a passage for the actual beam only, still accounting for the screen thickness and a constant 20° slant.

The elliptic covers are held in place by small and strong permanent magnets inserted in the screen central piece. To achieve their removal and repositioning, a “permanent electro-magnet” (PEM) is used, i.e. a permanent magnet that can be deactivated by powering the surrounding coil. This PEM is mounted on a small wagon running on two rails parallel to the main axis of the screen thanks to an indented belt forming a closed loop. An additional on-board mechanism allows it to move up and down from approximately 3 cm, in order to extract and replace the covers. To ensure a reliable lifting, a mechanical “extractor” was added, using four screw-like pins that get inserted in four slots carved in each cover, shown on Figure 5(a); centering pins were added as well on protruding fingers to ensure a reliable positioning. An extra shift was implemented for the wagon movements to allow the extraction system to have a secure grip on the covers.
The limitations in the rails length made it impossible for this extractor to reach the tip cover. Its handling thus required an additional PEM device, together with some extra commands.

*(a) Screen covers*

*(b) Wagon and steering rails*

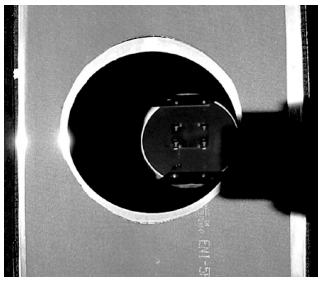

*(c) Obstructing cover*

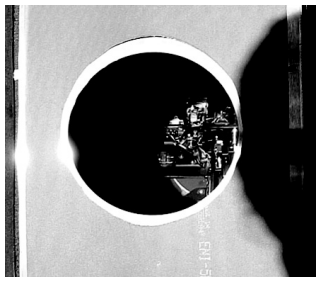

*(d) Extraction*

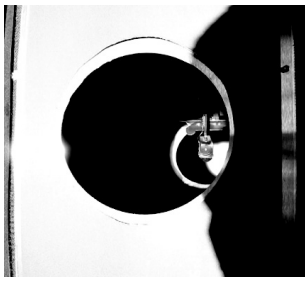

*(e) Removal*

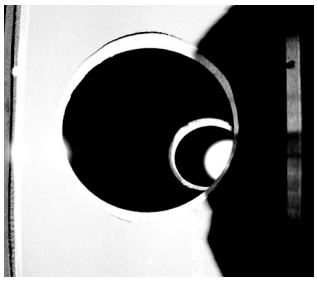

*(f) Illumination*

*Figure 5: Motorized screen with removable covers for incident beam path.*

The wagon is driven by a stepping motor, controlled by a specific ISEL micro-controller with a RS-232 interface. A typical cycle of extraction, removal and replacement of a cover is sequenced as follows:

- Wagon moved above the appropriate cover, PEM deactivated and lowered, then activated again to retrieve the cover by lifting it up;

- Wagon positioned out of the beam path and kept in place as long as needed to complete the image acquisition and processing phase;
- Wagon moved back above the open hole, PEM lowered, deactivated then lifted up empty, the cover being back in place.

Once the wagon movements were adequately calibrated to position it right above each cover, this new design was tested successfully with hundreds of random extractions at different screen inclinations.
The definitive screen panel is shown on Figure 5(b), where the wagon is in position to remove the tip cover and where all other covers are missing. Figures 5(c) to 5(f) illustrate the sequence of events taking place when the projection screen obstructs the incident beam path.

## BRDF results and validation

As detailed in Andersen (2002), three types of graphical representations were developed to provide various visualization possibilities of the transmitted or reflected light distribution features, in addition to a recombined view of the six calibrated images, gathering the latter into a unique orthogonal projection:

- the projection of the BT(R)DF values on a virtual hemisphere, allowing a precise analysis of the angular distribution;
- a photometric solid, representing the BT(R)DF data in spherical coordinates with growing radii and lighter colors for higher values, illustrated in Figure 6;
- several section views of this solid, providing an accurate display of the numerical values distribution.

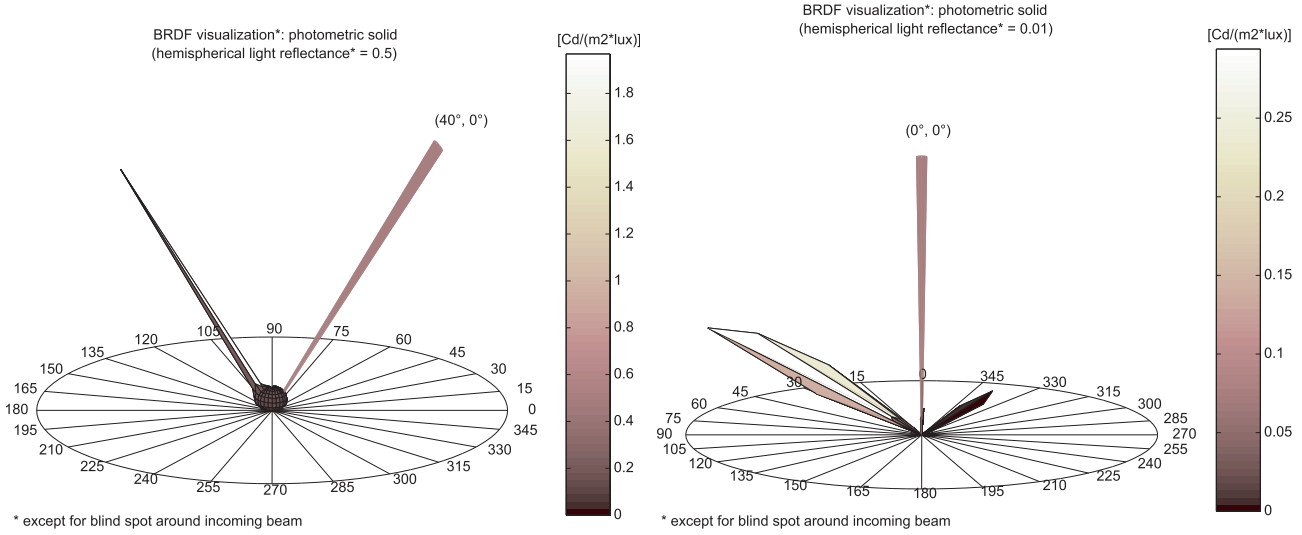


*(a) Opalescent plexiglas, ($\theta_1$, $\phi_1$) = (40°, 0°)* *(b) Holographic film (HOE), ($\theta_1$, $\phi_1$) = (0°, 0°)*

*Figure 6: BRDF representation as a photometric solid.*

An in-depth validation of both BTDF and BRDF was conducted, based on different approaches (Andersen, 2004):

- assessment of error at each intermediate stage of calibration and processing, a final error being deduced;

- bidirectional measurements of systems presenting a known symmetry and verification against standard luminance-meter data or analytical calculations;
- empirical validation based on bidirectional measurements comparisons between different devices; in case of disagreement, however, no conclusion can be established;
- assessment of hemispherical optical properties by integrating BT(R)DF data over the whole hemisphere and comparison to Ulbricht sphere measurements (Commission Internationale de l'Eclairage, 1998);
- comparison of monitored data with ray-tracing simulations to achieve a higher level of details in the BT(R)DF behaviour assessment.

These studies led to a relative error on BT(R)DF data of only 10%, allowing to confirm the high accuracy and reliability of this novel device.

## Conclusions

This paper presents the conception and construction of an innovative, time-efficient bidirectional goniophotometer based on digital imaging techniques and combining BTDF and BRDF assessments. To allow reflection measurements, a controlled passage of the incident beam into the measurement space was created, minimizing parasitic reflections around the sample. Openings in the detection screen for the situations where it obstructs the incoming light flux were also required, made as small as possible to restrict the produced blind zones; to remove these elliptic covers, a motorized extraction and repositioning system was developed and tested successfully.
This design proved efficient and reliable, for both the light beam penetration into the measurement space and the passage through the obstructing screen. The high accuracy achieved for BTDF assessments was checked to be kept for BRDF measurements as well, placing reliance on the assumptions made in the construction of the instrument.

## Acknowledgements

This work was supported by the Swiss Federal Institute of Technology (EPFL) and the Commission for Technology and Innovation (CTI). The authors wish to thank Pierre Loesch and Serge Bringolf for their contribution in the photogoniometer's mechanical development.

## References

Andersen, M. (2002). Light distribution through advanced fenestration systems. *Building Research and Information*, 30(4):264–281.

Andersen, M. (2004). *Innovative bidirectional video-goniophotometer for advanced fenestration systems*. PhD thesis, EPFL, Lausanne.

Andersen, M., Michel, L., Roecker, C., and Scartezzini, J.-L. (2001). Experimental assessment of bi-directional transmission distribution functions using digital imaging techniques. *Energy and Buildings*, 33(5):417–431.

Apian-Bennewitz, P. and von der Hardt, J. (1998). Enhancing and calibrating a goniophotometer. *Solar Energy Materials and Solar Cells*, 54(1-4):309–322.

Aydinli, S. (1996). Short description of the spiral goniophotometer for bi-directional measurements (TU Berlin). Report for IEA SHC Task 21, ECBCS Annex 29, Subtask A, Technische Universität Berlin (TUB), Berlin.

Bakker, L. and van Dijk, D. (1995). Measuring and processing optical transmission distribution functions of TI-materials. Private Communication, TNO Building and Construction Research, Delft.

Breitenbach, J. and Rosenfeld, J. (1998). Design of a Photogoniometer to Measure Angular Dependent Optical Properties. In *Proceedings of International Conference on Renewable Energy Technologies in Cold Climates*, pages 386–391, Ottawa, Canada. Solar Energy Society of Canada Inc.

Commission Internationale de l'Eclairage (1977). Radiometric and photometric characteristics of materials and their measurement. *CIE*, 38(TC-2.3).

Commission Internationale de l'Eclairage (1998). Practical methods for the measurement of reflectance and transmittance. *CIE*, 130.

Papamichael, K., Klems, J., and Selkowitz, S. (1988). Determination and Application of Bidirectional Solar-Optical Properties of Fenestration Materials. Technical Report LBL-25124, Lawrence Berkeley National Laboratory, Berkeley.